Pure appl. geophys. 154 (1999) 513–540
0033–4553:99:040513–28 $ 1.50 0.20:0

Pure and Applied Geophysics

Geologic Setting, Field Survey and Modeling of the Chimbote, Northern Peru, Tsunami of 21 February 1996

JOANNE BOURGEOIS,[1] CATHERINE PETROFF,[2] HARRY YEH,[2] VASILY TITOV,[3,4] COSTAS E. SYNOLAKIS,[4] BOYD BENSON,[5] JULIO KUROIWA,[6] JAMES LANDER,[7] and EDMUNDO NORABUENA[8]

Abstract—Whereas the coast of Peru south of 10°S is historically accustomed to tsunamigenic earthquakes, the subduction zone north of 10°S has been relatively quiet. On 21 February 1996 at 21:51 GMT (07:51 local time) a large, tsunamigenic earthquake (Harvard estimate M_w 7.5) struck at 9.6°S, 79.6°W, approximately 130 km off the northern coast of Peru, north of the intersection of the Mendaña fracture zone with the Peru–Chile trench. The likely mechanism inferred from seismic data is a low-angle thrust consistent with subduction of the Nazca Plate beneath the South American plate, with relatively slow rupture characteristics. Approximately one hour after the main shock, a damaging tsunami reached the Peruvian coast, resulting in twelve deaths. We report survey measurements, from 7.7°S to 11°S, on maximum runup (2–5 m, between 8 and 10°S), maximum inundation distances, which exceeded 500 m, and tsunami sediment deposition patterns. Observations and numerical simulations show that the hydrodynamic characteristics of this event resemble those of the 1992 Nicaragua tsunami. Differences in climate, vegetation and population make these two tsunamis seem more different than they were.

This 1996 Chimbote event was the first large ($M_w > 7$) subduction-zone (interplate) earthquake between about 8 and 10°S, in Peru, since the 17th century, and bears resemblance to the 1960 (M_w 7.6) event at 6.8°S. Together these two events are apparently the only large subduction-zone earthquakes in northern Peru since 1619 (est. latitude 8°S, est. M_w 7.8); these two tsunamis also each produced more fatalities than any other tsunami in Peru since the 18th century. We concur with PELAYO and WIENS (1990, 1992) that this subduction zone, in northern Peru, resembles others where the subduction zone is only weakly coupled, and convergence is largely aseismic. Subduction-zone earthquakes, when they occur, are slow, commonly shallow, and originate far from shore (near the tip of the wedge). Thus they are weakly felt, and the ensuing tsunamis are unanticipated by local populations. Although perhaps a borderline case, the Chimbote tsunami clearly is another wake-up example of a "tsunami earthquake."

Key words: Tsunami, subduction zone, seismicity, Peru seismicity, tsunami earthquake, tsunami sediments, tsunami modeling, Peru geology.

[1] Department of Geological Sciences, University of Washington, Seattle, WA 98195-1310, U.S.A.
[2] Department of Civil Engineering, University of Washington, Seattle, WA 98195-2700, U.S.A.
[3] Current Address: NOAA:PMEL, JISAO:University of Washington, Seattle, WA 98115, U.S.A.
[4] Department of Civil Engineering, University of Southern California, Los Angeles, CA 90089, U.S.A.
[5] GeoEngineers, Redmond, WA 98052, U.S.A.
[6] CISMID, Universidad Nacional de Ingenieria, Lima 27, Peru.
[7] CIRES, University of Colorado, Box 4409, Boulder, CO 80309, U.S.A.
[8] Instituto Geofisico del Peru, Apartado 13-0207, Lima, Peru.

Introduction

Peru has a written history of subduction-zone earthquakes and locally generated tsunamis retrospectively to the 16th century (elaborated in the following section), although the area of the Peru coast affected by the 1996 Chimbote subduction-zone earthquake and tsunami has a minimal historical record of such events. Beneath the coast of Peru the Nazca Plate is subducted at a moderately oblique angle (convergence rate estimated to be 7–8 cm:yr by various techniques; e.g., see NORABUENA *et al.* (1998); see also SPENCE *et al.*, SWENSON and BECK, this volume) beneath the South American plate, forming the Peru–Chile trench. Oligocene (30 m.y. old) oceanic crust is being subducted beneath northern Peru, while Eocene-age (40 m.y.) crust is being subducted south of the Mendaña fracture zone, which intersects the trench at about 10–11°S (Fig. 1). Onshore gravity measurements indicate that the angle of the subducting slab, bounded by the Carnegie Ridge to the north (off Ecuador) and the Nazca Ridge to the south (Fig. 1), is particularly shallow (DEWEY and LAMB, 1992); there is a paucity of onshore volcanism associated with this zone.

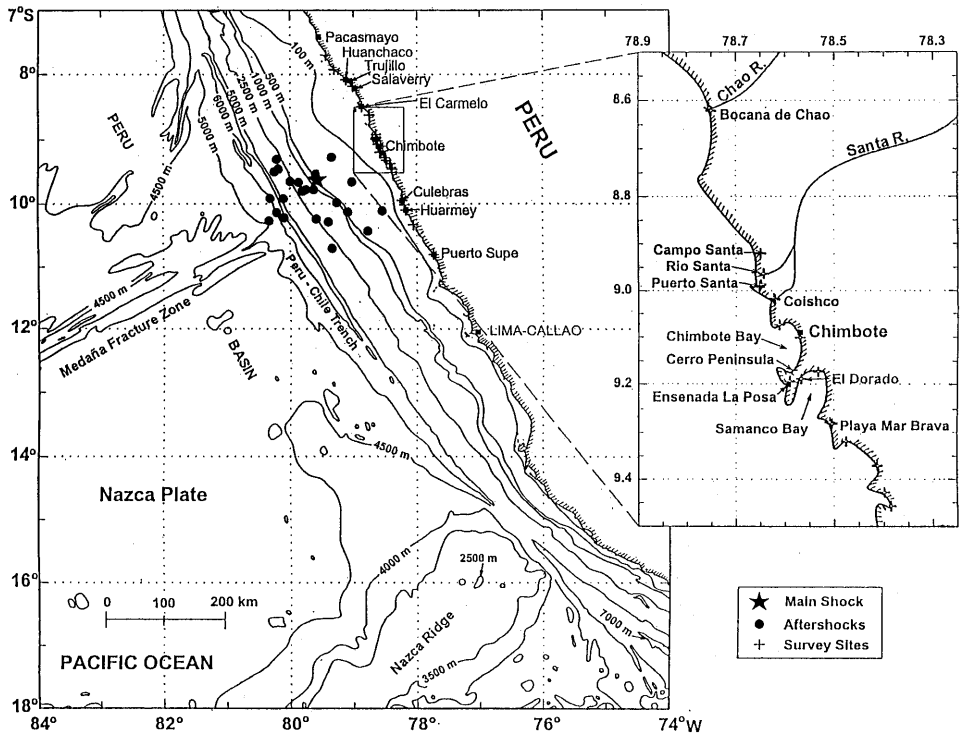

Figure 1
Maps of the Peruvian coastal region and the vicinity of Chimbote. The epicenter of the main shock is marked with a star; aftershocks are marked with an O. Main shock and aftershock locations (21 February to 6 April 1996) from the U.S. National Earthquake Information Center (USGS).

The northern Peru subduction zone has not been studied in detail, but its characteristics agree in general with a Wadati–Benioff zone in *central* Peru that is geometrically well constrained, as proposed by the horizontal subduction model of HASEGAWA and SACKS (1981) (LINDO *et al*., 1992; NORABUENA *et al*., 1994). The slab in central Peru dips at an angle of 30° and at about 100-km depth bends to become subhorizontal. NORABUENA *et al*. (1998) discuss the partitioning of Nazca-South America convergence of the central Andes region, assigning about 50% to the locked plate interface, and about 25% to Andean crustal shortening.

The area affected by the Chimbote tsunami is also within a coastal region with no evidence of late Cenozoic uplift. Whereas far northern and southern Peru are characterized by flights of uplifted marine terraces (DE VRIES, 1988; HSU *et al*., 1989; MACHARE and ORTLIEB, 1992), Peru's coastline from about 7°S to 13°S lacks such terraces. Is this lack of terraces indicative of a relative lack of interplate coupling (suggested by an anonymous reviewer)? A particularly well-studied part of the north-central coastline is the Rio Santa delta and coastal plain (WELLS, 1996), near the center of the tsunami-affected area, around 9°S. This delta exhibits evidence of beach-ridge accretion over the last 6000 years, and no more than about 1 m of relative sea-level change during that same interval (WELLS, 1996), consistent with global estimates of equatorial sea-level changes (TUSHINGHAM and PELTIER, 1991).

Bathymetry and topography have significant large- and small-scale effects on tsunami behavior; the margin of Peru affected by this tsunami is quite variable in character (see, e.g., ATLAS DEL PERU, 1989). The Peru–Chile trench in this region is approximately 5-km deep and 200-km offshore. The Peruvian coastline is indented overall and is relatively straight from about 7°S to 14°S (Fig. 1). The shelf is particularly broad off Chimbote, narrowing dramatically south of 10°S, and more gradually north of 9°S. The region most affected by the 1996 tsunami (approximately 8 to 11°S) is characterized in the south by a rugged, irregular coastline, with bedrock exposures and pocket beaches, and in the north by long, low segments of accretionary coastal plain punctuated by rocky headlands. The geomorphic differences are at least partially due to greater river and sediment discharge in the northern region. Is this higher sediment supply related to the lower seismicity of this portion of the subduction zone?

Wave climate and oceanography also affect tsunamis, and the record they leave behind. With regard to the coastal wave climate of this part of Peru, typical swell is from the southwest, and longshore transport is correspondingly toward the north. The northward directed, cold Peru:Humboldt current dominates coastal oceanography and climate. There is a general absence of storms on this coastline, with only minor storm surges, typically less than 1 m. Tidal range is approximately 1 m; the tsunami struck at about mid-tide, on an outgoing tide. A storm surge (or meteorological tide) of approximately 15 cm, along with heavy swell, was reported to us to be present during the 1996 tsunami, and some larger ships had been

evacuated (prior to and unrelated to the tsunami) from harbors due to these conditions. Civil defense experts in Peru attribute the relatively low damage and fatality from the Chimbote tsunami to the precautions already taken due to storm swell.

The El Niño phenomenon causes a well-known, geologically and historically documented disruption in climate and circulation along the coast of Peru (e.g., see WELLS, 1990). The term El Niño originated in this region, and most recent El Niño years are 1982:83 and 1997:98. In addition to the change in ocean circulation during El Niño episodes, rainfall along this part of the coast may increase about ten-fold (to cms per year) during El Niño years. As will be discussed below, the possibility that the 1619 earthquake generated a significant tsunami is partly tied to this El Niño history.

The area affected by a tsunami is also influenced by local roughness due to vegetation, and the damage done is also clearly related to human habitation patterns. Climate plays a strong role in these factors. For example, although the (south) latitudes affected by the 1996 Chimbote event are very similar to the (north) latitudes affected by the 1992 Nicaragua tsunami (SATAKE *et al.*, 1993), coastal vegetation and habitation are very different at the two sites. Due to the extreme aridity of the Peru coast (typical rainfall <10 mm:yr), there is virtually no vegetation outside of the floodplains and deltas of rivers from the Andes. Irrigation has locally extended the area of vegetation cover, for example, on the Santa delta, which is irrigated for rice, potatoes, and other crops. Locally, indigenous shoreline plants (e.g., rushes) are present in patches along the Peru beaches; mangroves, abundant in Nicaragua, are absent in Peru due to low ocean temperatures. Due to the lack of vegetation in Peru, wind-blown coastal dunes are very common, and onshore tsunami effects are quickly reworked by the wind. Also, due to lack of trees and houses on the coast, it is rarely possible to measure maximum tsunami elevations, e.g., over a beach ridge.

Although population on the coast of Peru is sparse overall, the written history of tsunamis reverts to the 16th century. The Peruvian coast has been occupied, principally at or near river mouths, since about 10,000 years ago (CHAUCHAT, 1987). Adobe ruins, including large pyramids and the ancient city of Chan Chan, as well as irrigation structures and other signs of occupation, are present throughout the 1996 surveyed region. Irrigated agriculture and fishing continue to sustain the local economy; the cold Peru:Humboldt current generates the dry climate, mild ambient temperatures, and rich fishing grounds along the Peruvian coast. Chimbote is the largest port on the northern coast, providing a large protected embayment; it is the only heavily industrialized coastal city in the affected region. Virtually all coastal towns have fishing fleets, and a number have fish-meal factories and other industry associated with a fishing economy. A number of the affected towns are principally beach resorts.

History of Regional Earthquakes and Tsunamis

Based on aftershock distribution (Fig. 1), the rupture area of the 1996 Chimbote tsunamigenic earthquake was about 9.3°S to 10.3°S, an area not historically very active. Tsunamigenic events in Peru have struck primarily south of 12°S (e.g., see LOCKRIDGE, 1985). A short historical review of events between about 6°S and 12°S illustrates the unusual nature of the 1996 event, which affected an area less studied or prepared for local tsunamis.

Peru has a long-documented history of earthquakes and tsunamis (e.g., LOMNITZ, 1970; SILGADO, 1978; LOCKRIDGE, 1985; CARBONEL and AGUIJE, 1989; DORBATH *et al.*, 1990; PELAYO and WIENS, 1990; LANGER and SPENCE, 1995; SWENSON and BECK, 1996). LOCKRIDGE (1985) listed 34 tsunamigenic earthquakes off Peru from 1586 to 1974; of ten events producing destructive tsunamis, only the tsunamis from 1960 and 1966 occurred north of 12°S (Table 1). DORBATH *et al.* (1990) added (to Lockridge's compilation) two possible other tsunamigenic events in 1582 (17–18°S) and 1678 (Table 1) and revised some runup estimates. According to DORBATH *et al.* (1990), the three largest events in Peru ($M_w > 8.5$, tsunami runup > 10 m) occurred in 1604, 1746 and 1868; only the 1746 event is interpreted to have ruptured north of 12°S (Table 1). CARBONEL and AGUIJE (1989) catalogued earthquakes off the Peruvian coast from 1948 to 1986, including the 20 May 1978 tsunamigenic event (Table 1; Appendix A); they also summarized tsunami amplitude data from tide gauges at Callao (1952–1986) and Chimbote (1957–1986), from both near-field and far-field tsunamis.

DORBATH *et al.* (1990) subdivided the Peru subduction zone into three suggested segments (< 10°S; 10°–15°S; > 15°S), based on their catalogue of historical events, and characterized the northern segment as relatively aseismic. However, SWENSON and BECK (1996) reviewed the history of great earthquakes in Peru, Ecuador and Colombia, also providing a catalogue, and concluded that segmentation of this plate boundary, as defined by earthquakes in the 20th century, is not constant. In any case, the majority of destructive subduction-zone earthquakes and tsunamis in Peru have occurred in the central to southern region, south of 12°S, and most research and disaster planning has focused on this southern region (e.g., KUROIWA, 1995). The subduction zone from 10 to 14°S was quiet from 1746 to 1940, after which it generated four events (1940, 1942, 1966, 1974) (the 12 November 1996 event was at about 15°S); none is interpreted to have ruptured north of 10°S. Thus between about 7°S to 10°S there was a historical (subduction-zone) seismic and tsunamigenic gap dating back to at least 1619 (see Table 1). The November 1960 event (M_w 7.6) occurred at 6.8°S, at the northern end of the gap; PELAYO and WIENS (1990, 1992) denoted this 1960 event as an example of a tsunami earthquake. The 21 February 1996 event occurred at the southern end of that gap. Though not as destructive as many other historical events, the 1996 Chimbote tsunami produced more deaths than any other in Peru, with the possible

Table 1

Historical large and tsunamigenic, subduction-zone earthquakes, Peru, between about* 6 *and* 12 *degrees South*[1]

Date	M_s (est.)	M_w (est.)	Latitude (S)	Longitude (W)	Est. lat. range (°S)	Rupture length km (est.)	Focal depth km (est.)	MMI (max)	M_t	Runup max (m)
19:II:1619	na	7.8	7.7–8.0	na	na	100–150	na	X	na	na
17:VI:1678	na	7.7–8.0	10.0–11.0	na	10.0–11.0	100–150	na	IX	8.5	5
25:I:1725	na	7.5	10.0–11.0	na	10.0–11.0	75	na	VIII	none	none
28:X:1746	8.0–8.4	8.6–9.5	12	77	10.0–13.0	350	na	X	9.2	15–24
24:V:1940	7.9–8.4	8.1–8.2	10.5	77	10.3–12	100–180	60	VIII	8.2	2.0–3.0
20:XI:1960	6.75	7.6	6.7	80.9	na	100	9	na	7.75	9**
17:X:1966	7.8–8.0	7.7–8.1	10.7	78.8	10.0–11.0	100	40	VIII	8.2	2.6–3
31:V:1970*	6.6–7.7	7.9	9.2	78.8	9.5–10.5	130	43	IX	na	0.5–1.8
3:X:1974	7.6–8.1	7.9–8.0	12.3	77.7	11.8–13.2	140–180	13	VIII	7.9	1.6–1.8
20:V:1978	5.5	5.9	10.3	78.6	na	na	50	na	na	1.5
21:11:1996	6.7	7.5	9.62	79.6	9.3–10.3	100	15	IV	7.8	5

[1] Principal sources: DORBATH *et al.* (1990); LOCKRIDGE (1985); SWENSON and BECK (1996); also CARBONEL and AGUIJE (1989); PELAYO and WIENS (1990); Harvard CMT catalogue, and this study.

* 1970 earthquake(s) occurred not along the subduction zone, but in the downgoing slab (BECK and RUFF, 1989).

** "Some nine meters high" reported in SILGADO (1979); questionable accuracy; see Appendix A.

na not available; M_s surface wave magnitude; M_w moment magnitude; MMI Modified Mercalli Scale magnitude; M_t tsunami magnitude of Abe, based on teletsunami runup.

exception of the November 1960 event, since the 18th century. The 1970 earthquake series in northern Peru, which led to more than 50,000, perhaps 70,000 deaths—including the Huascaran slide catastrophe—and generated a tsunami, has been interpreted as a normal-fault (intraplate) event in the downgoing slab, with a large reverse-fault aftershock to the south (BECK and RUFF, 1989).

Although a number of authors have compiled catalogues of earthquakes and tsunamis for Peru, none is complete for the northern coast. Thus we present a summation of historical subduction-zone and tsunamigenic earthquakes in northern Peru in Appendix A (see also Table 1), illustrating the rarity of interplate events (1619, 1960, 1996) north of 10°S. DORBATH *et al.* (1990) did not list the 1960 event and noted that large subduction-zone events in Peru have been limited to the region south of 10° (south of the Mendaña fracture zone), with the possible exception of the 1619 earthquake that destroyed Trujillo. This 1619 event, whose seismic character is a matter of speculation, also has no known written record of a tsunami. However, the northern coast would have been very sparsely populated, therefore a tsunami may not have been reported. SILGADO (1978) reports an account of inundation by muddy water at some coastal towns, attributed to river flooding, although suggestive to us of a tsunami. WELLS *et al.* (1987) speculated that a distinctive wood-debris line on the Santa delta plain was deposited by a tsunami, most likely from this event. They suggested the date of 1618, based on radiocarbon dating and a recorded El Niño, which they argued was necessary to bring the observed tropical wood from the north (normal-year currents are from the south). We reason that this wood could have sat on the beach for a year or more, however, and then have been transported by a tsunami in 1619 or somewhat later.

The 1996 Chimbote Earthquake and Aftershocks

The main shock (M_s estimates 6.6–6.7, M_w estimates 7.3–7.5) occurred on 21 February 1996, at 12:51 GMT (07:51 local time), at 9.6°S, 79.6°W, approximately 130 km off the coast of northern Peru (Fig. 1). The Harvard CMT solution indicates a low-angle thrust, consistent with subduction of the Nazca Plate beneath the South American Plate, with relatively slow rupture characteristics (EKSTRÖM and SALGANIK, 1996; NEWMAN and OKAL, 1996). Aftershocks (late February through early April 1996) of magnitude 5.1 or lower occurred in a region from the outer shelf to the trench (Fig. 1). Overall the aftershock area is blocky rather than elongated, but more or less parallel to the trench and the Peruvian coastline.

The preferred focal mechanism reported by Harvard CMT is strike 335°, dip 14°, rake 88°, with alternative solution, strike 157°, dip 76°, rake 91°. The main pulse lasted approximately 30 seconds (max. peak 50.25 10^{17} Nm:sec) with an M_w of 7.2 after 32 seconds; the second pulse continued for at least the next half minute

Table 2

21 February 1996 Chimbote, Peru earthquake intensity (Modified Mercalli Scale), as reported by eyewitnesses to tsunami surveyors, March, 1996

Surveyed towns	Lat.	Long.	MM intensity
Puerto Supe	S: 10:48.034	W: 77:44.06	II–III (JB, JK)
B. Tomborero	S: 10:19.566	W: 78:3.186	I (JB)
Huarmey	S: 10:5.882	W: 78:10.185	III, IV, IV, IV (JK)
Playa Chimus	S: 09:19.161	W: 78:28.524	I (II?) (JB)
El Dorado	S: 09:11.294	W: 78:33.981	II (JB)
Coishco	S: 09:1.161	W: 78:37.223	III, III, III (JK)
Puerto Santa	S: 08:59.472	W: 78:39.109	I, II (JK)
Campo Santa	S: 08:55.175	W: 78:38.946	II–III (JB)
Salaverry (port of Trujillo)			I(JK)
Las Delicias 2	S: 08:11.145	W: 79:0.64	I, II (JB)
La Posa Huanch.	S: 08:5.169	W: 79:7.358	I (JB)
Huaca Prieta	S: 07:55.419	W: 79:18.444	(strongly felt? unreliable)
Puerto Chicama	S: 07:41.914	W: 79:26.256	I ($\sim$15 people, JB)
Pacasmayo			I, I, I (II?) (JB)

(JB J. Bourgeois; JK J. Kuroiwa).

(max. peak 13.47 10^{17} Nm:sec.). Based on teleseismic energy estimates, NEWMAN and OKAL (1996) interpreted this event to have been intermediate in source slowness between regular events and "tsunami earthquakes" have performed a more thorough analysis of this earthquake.

Based on far-field tsunami amplitudes recorded by tide gauges, ABE (1996) estimated the tsunami magnitude for the Chimbote event to be M_t 7.8 (see ABE, 1979, 1981; also OKAL, 1988). The substantial discrepancy among the values of M_s, M_w, and M_t also suggests that this event can be characterized as a "tsunami earthquake." The term "tsunami earthquake" was introduced by KANAMORI (1972), and may be defined as an earthquake that generates a tsunami significantly greater than expected based on the value of M_s (see also, e.g., PELAYO and WIENS, 1992). Consequently, such tsunamis often induce greater damage and casualties because local populations are not alarmed by the earthquake, and improper and:or no warnings may be issued due to insignificant ground-shaking associated with the earthquake. Indeed, based on our eyewitness interviews, along the coast, the maximum Modified Mercalli Intensity (MMI) was IV (Table 2). Many eyewitnesses did not feel the earthquake; the shaking, where felt, was mild. In general, the earthquake was felt more strongly to the south of Chimbote than to the north. Even in Chimbote—closest to the epicenter and worst hit by the tsunami—the shaking was not noticed by everyone.

Tides and Tide-gauge Records

The tsunami on 21 February arrived at approximately mid-tide, on an outgoing tide. Throughout the surveyed region normal tidal range is between about 0.7 and 1.1 m. Using local tide tables, we corrected runup measurements by noting the date and time of day of the field measurement, and correcting to the tide level at the estimated time of arrival of the tsunami on 21 February (see Table 3). Note that these measurements are rated A, B, C based on reliability. Due to possible errors in field measurement, in estimates of water level at the time of survey, in estimates of time of the tsunami arrival, and in use of tide tables, error on our corrected measurements is probably about ± 30 cm, in some cases more. Also, Navy officers reported to us that there was a storm surge in the region at this time. For example, on 16 February the port of Chimbote was partially closed, due to large swells, and eight large ships were sent out to a deeper area; only two large ships were in mooring on 21 February. The hydrographic office reported to us a meteorological high tide of one-half foot on 21 February. We chose not to correct for this meteorological tide; if this surge was consistent throughout the time and area surveyed, each of our corrected measurements would be about 15 cm too high.

Tidal records for the day of the tsunami were obtained on site from tide-gauge stations at the Peruvian ports of Salaverry and Chimbote, and later via the Pacific Tsunami Warning Center from Callao, Easter Island, and other localities. Figure 2 displays tide-gauge records of the tsunami from Chimbote and Salaverry, both recovered during our survey from tube-type gauges with a two-inch bottom orifice and a float for mechanical registry of the tide level. In both cases, the first obvious record of the tsunami is an upward motion, however in both cases, a first downward motion is possible, though difficult to discern from the printed record. Eyewitnesses and reports from nine localities, including Puerto Supe, the Chimbote area, and La Posa Huanchaco, near Salaverry, noted the water going out first, approximately 50–100 meters horizontally (estimated in civil defense reports, pointed out to our teams by eyewitnesses in two cases). Such observations would be consistent with a first downward motion of approximately half a meter, and such a drop could be present on tide-gauge records, but be small enough not to be obvious.

At Chimbote, the gauge is located on a spur of the northernmost pier in the port called Enapu. The port had been closed for the five days preceding the tsunami, due to high waves, which are evident in the small fluctuations preceding tsunami arrival (Fig. 2a). The gauge record shows the first upward spike of the tsunami at about 09:06 local time, when tidal elevation was 1.6 m above MLLW and falling; this upward spike, on the original record, does appear to be preceded by a smaller (30–50 cm?) downward motion. The gauge indicator rose to a level of 2.7 m and remained pegged at that level for half an hour (no data for that period were plotted in Fig. 2a). At this time the 1000-m-long Enapu pier was inundated for the

Table 3

February 1996 Peru tsunami runup measurements (south to north)

Location (local name)	Corr. R_{max} (m)	L_{max} (m)	Corr. R'_{max} (m)	Rating	Date	Time local	Latitude Deg.	Latitude Min.	Longitude Deg.	Longitude Min.	R_{max} (m)	R'_{max} (m)	Corr. (m)
Puerto Supe	1.94			C	3/17/96	11:22	S: 10	48.034	W: 77	44.06	1.89		0.05
Balnearia Tomborero	1.01	50	1.33	C	3/23/96	9:53	S: 10	19.566	W: 78	3.186	0.91	1.23	0.1
Huarmey	0.89	65	1.3	B	3/17/96	14:00	S: 10	5.882	W: 78	10.185	0.44	0.85	0.45
Tuquillo	1.93	25	1.97	A	3/17/96	15:20	S: 10	1.071	W: 78	11.578	1.38	1.42	0.55
Culebras I, bluff	5.04		3.6	B	3/17/96	17:00	S: 09	57.023	W: 78	13.814	4.59	3.15	0.45
Culebras II, dock	3.35			B	3/17/96	17:00	S: 09	56.886	W: 78	13.674	2.9		0.45
Puerto de Casma	2.25			C	3/22/96	11:45	S: 09	27.444	W: 78	23.124	2.6		−0.35
Pinos	1.6		1.6	B	3/22/96	10:45	S: 09	25.712	W: 78	23.9	1.8	1.8	−0.2
Playa Tortuga	2.42			B	3/22/96	9:20	S: 09	22.216	W: 78	24.771	2.47		−0.05
Playa Chimus	3.13	112		A	3/22/96	12:30	S: 09	19.161	W: 78	28.524	3.48		−0.35
Playa Mar Brava I	2.38	90	2.75	B	3/22/96	10:20	S: 09	16.804	W: 78	30.206	2.53	2.9	−0.15
Playa Mar Brava II	2.08	174	3.8	A	3/22/96	10:10	S: 09	16.646	W: 78	30.51	2.23	3.95	−0.15
Ensenada La Posa IV (E)	4.5	64		A	3/22/96	16:20	S: 09	11.663	W: 78	34.866	4.25		0.25
Notch NW of Ens. La Posa	3.84	80		A	3/22/96	16:00	S: 09	11.663	W: 78	34.866	3.67		0.15
Ensenada La Posa I	4.13	24		A	3/22/96	15:00	S: 09	11.646	W: 78	34.666	4.18		−0.05
Ensenada La Posa III	4.35	24		A	3/22/96	15:35	S: 09	11.622	W: 78	34.773	4.3		0.05
Ensenada La Posa II, boat ramp	3.61	54		A	3/22/96	15:10	S: 09	11.57	W: 78	34.687	3.66		−0.05
El Dorado I	2.78			A	3/21/96	17:35	S: 09	11.3	W: 78	34	2.23		0.55
El Dorado II		350	2.1	B	3/21/96	18:15	S: 09	11.294	W: 78	33.981		1.6	0.5
Playa Alconsillo	1.69	130		A	3/21/96	16:10	S: 09	10.366	W: 78	31.938	1.39		0.3
Chimbote Bay	2.8	64		B	3/21/96	9:35	S: 09	6.058	W: 78	34.17	2.9		−0.1
Port of Chimbote I, guardshack	3.04	40		A	3/21/96	10:00	S: 09	4.424	W: 78	36.701	3.24		−0.2
Port of Chimbote II, pier	4.89			A	3/21/96	10:15	S: 09	4.424	W: 78	36.701	5.14		−0.25

Table 3 (*Continued*)

Location (local name)	Corr. R_{max} (m)	L_{max} (m)	Corr. R'_{max} (m)	Rating	Date	Time local	Latitude Deg.	Latitude Min.	Longitude Deg.	Longitude Min.	R_{max} (m)	R'_{max} (m)	Corr. (m)
Coishco III, street, fish market	2.2	90	3.25	A	3:18:96	8:00	S: 09	1.161	W: 78	37.223	2.6	3.65	0.4
Coishco II, pumphouse	2.6	90		A	3:18:96	8:00	S: 09	1.02	W: 78	37.273	3		0.4
Coishco I (wall)	4.7	87		C	3:18:96	7:45	S: 09	0.958	W: 78	37.37	5.05		0.35
Puerto Santa III, transit line	1.75	330		A	3:18:96	14:00	S: 08	59.472	W: 78	39.109	1.3		0.45
Puerto Santa II	2.68	112	3.28	A	3:18:96	14:55	S: 08	59.261	W: 78	39.057	2.08	2.68	0.6
Puerto Santa I	1.68	138	3.15	A	3:18.96	14:10	S: 08	59.172	W: 78	38.918	1.23	2.7	0.45
Rio Santa III	2.7	222	3.18	A	3:18:96	17:10	S: 08	57.782	W: 78	38.592	2.25	2.73	0.45
Rio Santa II	2.3	380		A	3:21:96	10:30	S: 08	57.764	W: 78	38.595	2.6		0.3
Rio Santa I	3.1	364		A	3:21:96	10:30	S: 08	57.764	W: 78	38.595	3.4		0.3
Campo Santa	1.21	455	1.35	A	3:21:96	17:45	S: 08	55.175	W: 78	38.946	0.66	0.8	0.55
Bocana de Chao II	1.78	259	2.72	A	3:20:96	17:15	S: 08	37.268	W: 78	45.006	1.18	2.12	0.6
Bocana de Chao I	1.41	256		B	3:20:96	17:40	S: 08	36.909	W: 78	45.236	0.86		0.55
El Carmelo I	1.2	113	2.6	A	3:19:96	14:20	S: 08	29.234	W: 78	52.317	0.7	2.1	0.5
Las Delicias II	2.7	20	2.88	B	3:19:96	18:00	S: 08	11.145	W: 79	0.64	2.2	2.38	0.5
Las Delicias I	3.09	17	3.29	B	3:19:96	17:30	S: 08	10.986	W: 79	0.786	2.54	2.74	0.55
La Posa Huanchaco	3.76	73		B	3:20:96	11:20	S: 08	5.169	W: 79	7.358	3.46		0.3
Huanchaco	3.1			C	3:20:96	11:20	S: 08	4.636	W: 79	7.212	2.8		0.3
Huaco Prieta		28	2.02	C	3:19/96	17:20	S: 07	55.419	W: 79	18.444		1.42	0.6
Puerto Chicama	1.54	59		C	3:19:96	14:30	S: 07	41.914	W: 79	26.256	0.99		0.55

Table explanations: (see text for notes on corrections) Corrected R_{max}—local runup maximum at point of local maximum inundation; L_{max}—local maximum horizontal inundation (from shoreline); Corrected R'_{max}—local elevation of tsunami, other than at maximum inundation.

Rating: A, very reliable physical evidence, corroborated or judged very reliable; B, moderately reliable, based on physical evidence and:or eyewitness; C, questionable physical or eyewitness evidence.

R_{max}, R'_{max}, corr.—original measurements, with corrections from tide tables (see text).

landward 800 m of its length; a small red pickup truck on the pier was reportedly carried about 10 m horizontally and turned over but did not fall in the water. A 2-m-high guard shack controlling pier access on land was destroyed and the guard was seriously injured. Our measured maximum local runup height was 4.9 m. The remainder of the Chimbote record shows oscillations gradually decaying over the next 24 hours.

The tide gauge for the port of Salaverry (port of Trujillo, Fig. 1b) is located on a north-facing pier inside the port. No tsunami damage was reported; this port had also been closed because of swell. Tidal variation at Salaverry is approximately 1.1 m. The tide-gauge record shown in Fig. 2b exhibits a sharp upward spike of 0.75 m at approximately 09:07, followed by a downward excursion of at least 0.65 m (from the 09:07 tide level). The first upward stroke is not obviously preceded by downward motion greater than the noise on the record. On the downward

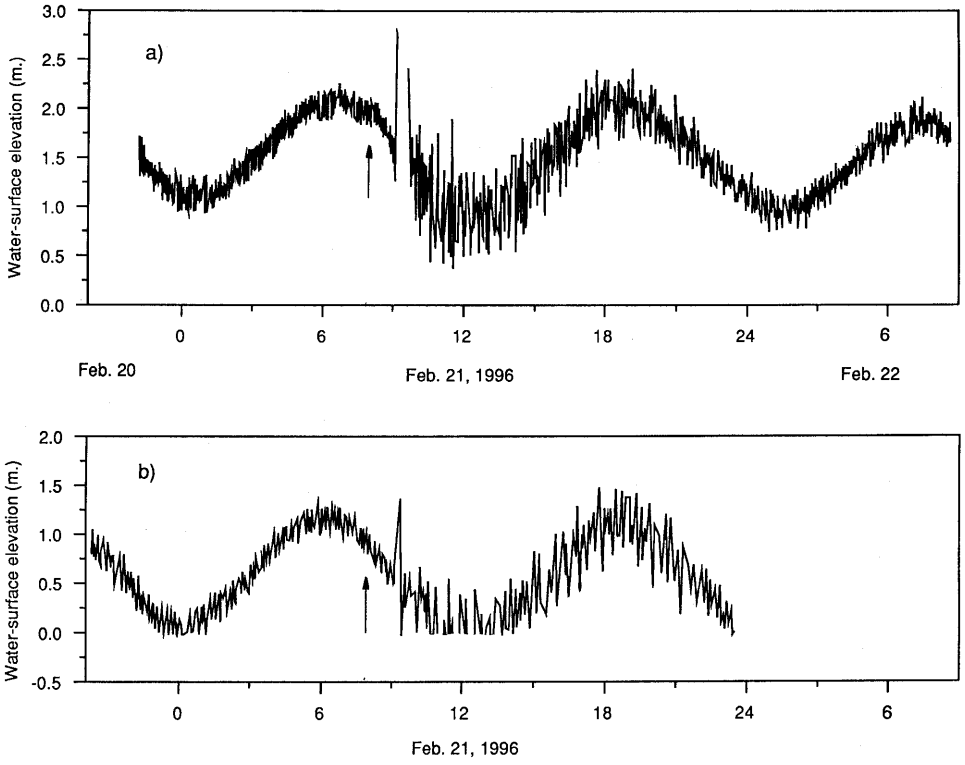

Figure 2

The tide-gauge records from (a) Chimbote and (b) Salaverry (which have been digitized, based on originals supplied to us by port captains). The earthquake occurred at 07:51 local time (marked by vertical arrow). The datum of water surface elevation in each record is arbitrary. At Chimbote, the data from 09:11 to 09:39 A.M. are missing. At Salaverry, the water surface levels lower than 0 meter were not recorded.

stroke, the pen went off scale, so that the maximum wave height, or peak-to-trough amplitude, of the tsunami in the port is not known.

The tide gauge at Callao (La Punta, the port of Lima, Peru; Fig. 1b) is reported to be a stilling well (encoder). The record at Callao for 21 February is incomplete, with missing data from 15:36 to 18:55 GMT (10:36 to 13:55 local time), during which the elevation of the recorder changed by 0.44 m (this change is consistent with the normal dropping tide). The first large excursion on the record occurs just before 10:00 local time and is downward, approximately 0.3 m, followed by an upward motion of about 0.4 m. The next downward motion of about 0.6 m is the maximum excursion before the gap in the record. After the gap, at about 19:15 (14:15 local), there is an excursion of about 0.7 m.

Other tide gauges in the Pacific recorded the following (maximum peak-to-trough amplitudes): Easter Island, Chile: 0.6 m; Santa Cruz, Galapagos (Ecuador): 0.4 m; Socorro, Mexico: 0.25 m; Hilo, HI (USA): 0.2 m; Kahului Maui, HI (USA): 0.3 m. HEINRICH *et al.* (1998) report that the tsunami was barely discernible on many other Pacific tide records, but that it may have reached a height of 2 m on Hiva-Oa, in the Marquesas Islands. The tsunami was not recorded in Japan.

Damage and Casualty Reports

According to the Institute for National Civil Defense in Peru, 12 people died in the tsunami and 57 were injured; 375 required assistance, including 85 who were compensated for loss of crops. Fifteen houses were destroyed, 22 ''affected''; 2 boats were destroyed and 23 damaged. All along the affected area many temporary beach structures (kiosks) made of grass mats were swept away or damaged. Many boats were displaced, most dramatically from Samanco Bay south of Chimbote, where boats were displaced 300 m inland and remained beached there at the time of our survey. At Culebras, an unreinforced brick harbor wall was pushed over by the tsunami. At Coishco, some brick houses were damaged, several reinforced brick:concrete factory walls were partially destroyed, and 400 tons of fish meal stored behind a brick and concrete wall were damaged or destroyed. The fatalities including six line fishermen on the rocks at Coishco (Caleta Santa), four persons gathering firewood at the mouth of the Santa River, and two children on the beach looking for gold at Campo Santa. The Civil Defense reported that evacuation took place in the Chimbote area after the earthquake and as the water retreated on the morning of 21 February. All deaths were in isolated regions, and it is unknown whether tsunami victims felt the earthquake, knew if they did to expect a tsunami, or saw the tsunami coming.

Runup Observations

The runup survey covered over 500 km of coastline from Pacasmayo to Puerto Supe (Fig. 1; Table 3; Appendix B). The beaches are either wide, fairly plain and accretionary with very flat slopes (e.g., Campo Santa, Playa Mar Brava) or sheltered and curved, typically steep, and anchored by rocky outcrops (e.g., Ensenada La Posa). Because there is very little vegetation on the coast, and very few houses or other structures, runup observations were difficult and could not rely on the kinds of watermarks used for most recent events (see, e.g., SATAKE and IMAMURA, 1995). In Peru measurements were based primarily on evidence of shoreline debris lines above high tide, where not erased by wind. Eyewitness accounts, where independently confirmed or deemed to be reasonable, were also used.

Since the tide gauge of Chimbote saturated after the initial rise of the tsunami, and the Salaverry and Callao records are truncated, eyewitness reports are invaluable. The wave was generally described as black with no indications of breaking, occasionally with a hissing sound. Many recalled either two or three waves, usually in quick succession, with the second being the largest. The time between waves varied and at Coishco was reported near 8 min, at La Posa Huanchaco 9 minutes, at Playa Chimus 25 minutes. Many interviewees noted that during (and after) the tsunami the water became more turbulent, with bigger waves and a dirtier appearance. In El Dorado and Puerto Supe, eyewitnesses pointed to rocks and dock structures beyond which the water withdrew first. A number of eyewitnesses noted that the water remained high (or ponded) for 2–3 days.

Measured runup and tsunami elevations, corrected for tides, and also inundation distances, are shown in Figure 3 and compiled in Table 3. Most measurements were made with a leveling transit, relative to water level at the time of measurement; hand levels and tapes were used in some instances (see Appendix B). Latitude and longitude were determined by hand-held GPS and checked for consistency with local maps. Twelve topographic profiles, typically orthogonal to the shoreline, were measured at ten localities, in most cases with a leveling transit. These localities are: Bocana de Chao, Coishco, Huaca Prieta, La Posa Ensenada (three profiles), La Posa Huanchaco, Los Chimus, Pama Blanca, Playa Mar Brava, Puerto Chicama, and Rio Santa.

Most measurements are heights at maximum inundation distances ($R_{\max}$; the formal definition of tsunami runup) because no trees and few structures existed on beach ridges. When compared with other surveys, these numbers appear to underestimate the event because many reported runup elevations from other surveys are actually tsunami elevations on raised surfaces such as beach ridges (this is true, for example, of Nicaragua data; SATAKE *et al.*, 1993; ABE *et al.*, 1993). Where we did measure additional tsunami elevations, particularly if higher than $R_{\max}$, they are noted in Table 3 as $R'_{\max}$. The scatter in heights is typical of post-tsunami surveys

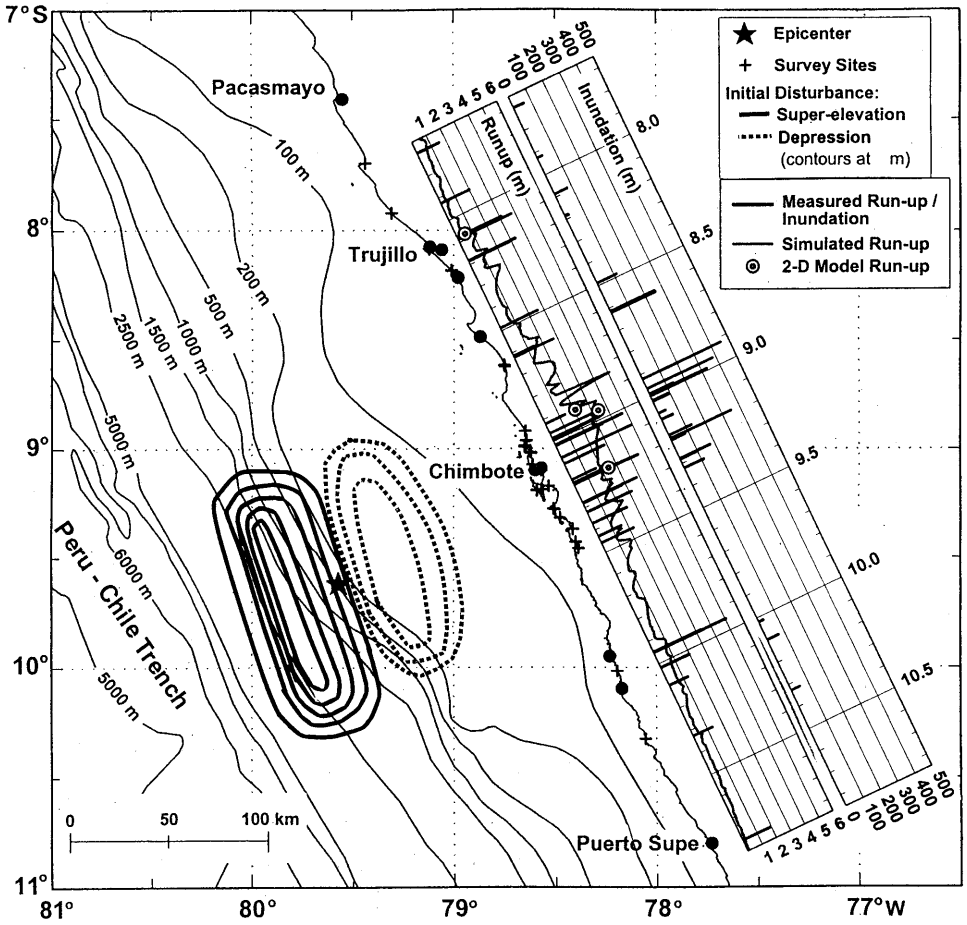

Figure 3
Tsunami runup heights and inundation distances along the Peruvian coast (see also Table 3; Appendix B). The values are from sea level at the time of tsunami arrival. Vertical bars represent (corrected) measured values; the continuous line and O represent numerically simulated values from a finer grid resolution (see text and Figure 4). The modeled displacement offshore (approximately located) is 1.8 m and 0.7 m, used as the initial sea-level displacement for the numerical model.

and is due to many factors, such as local differences in bathymetry and topography, presence or absence of vegetation (such as trees) and structures, and differences in reliability of data. Although the measured runup heights were not high except on steep slopes or walls, inundation distances were often quite large on low-sloping beaches. Several measured inundation distances were well over 200 m (see Fig. 3 and Table 3).

One of the remarkable tsunami runup effects was the inundation of a large tombolo 10 km south of Chimbote, separating Chimbote and Samanco bays (Figs.

1 and 3). The tombolo (low strip of land connecting the mainland with what would otherwise be an island), 1.5 km wide and 4.5 km long, is very flat at its west end, with many small sand dunes to the east near the mainland. The tsunami inundated this 1.5-km-wide flat area, from both sides; several small fishing boats were washed approximately 300 m inland from Samanco Bay. If one assumes a constant tsunami height of 1.5 m over Chimbote Bay, then, for the water to spread 750 m (halfway between the two bays) on the horizontal and frictionless dry beach, the classic dam-break theory (see, e.g., STOKER, 1957) predicts a time of almost 100 sec; therefore the tsunami must have had at least a 200 sec period. Friction is very important for such a thin-layer flow; hence the actual tsunami period would be markedly longer than this 200-sec lower-limit estimate.

There is a small rocky cove (Ensenada La Posa) on the other side of the attached island at the end of the tombolo. There is no vegetation or habitation in this cove, which faces directly to the tsunami; it has a 300-m-diameter circular shape with an 150-m narrow mouth and a 30° steep face up to 4 m high from the water level, then a gently sloping surface. Runup heights measured at four different locations were consistent at approximately 4 m, suggesting a gradual flooding motion without significant short-wave effects. These were the largest and perhaps the most representative values in this survey, as the beach is unobstructed and faces directly to the source.

Tsunami Deposits

Sand erosion, transport and deposition were observed throughout the affected region, although evidence was subtle and difficult to recognize due to the overall sandy and largely unvegetated coastline. Deposits were most apparent near river mouths where sand and mud were available for transport and where the beaches tended to be flat. Tsunami deposits were also more easily observed in these areas because the coastal plain typically has developed a soil surface, allowing deposits to be distinguished from underlying layers. Locally, the sand appeared to be normally graded and otherwise unstratified. Specific observations were made at Puerto Santa, Rio Santa, El Carmelo and Bocana de Chao. At the first two, profiles were measured and several trenches dug; sand samples were obtained at the latter two locations. Because all sites studied were supratidal and there is no observed or reported coseismic subsidence onshore, these tsunami deposits will likely be reworked and become unidentifiable within a few years.

At Puerto Santa, a very flat beach with 2-m runup height, the tsunami deposit comprised 4 to 11 cm of normally graded fine to very fine sand. We did not notice this deposit until trenches were dug into the vegetated surface and we could see that the sandy tsunami deposit had buried the bases of local plants (*Distichlis* and *Scirpus*), which were growing from the former (pre-tsunami) soil surface. The

deposit thickened in topographically low spots, thinning to zero at a distance of about 200 m from the shoreline.

On the cultivated fields north of the mouth of the Rio Santa, the tsunami deposit ranged from 0.6 to 1.6 cm thick. Very fine, locally rippled sand and silt were capped by up to 3 mm of mud, producing a normally graded layer (mud could be seen offshore in suspension near the mouth of the river). Inferred tsunami deposits were also observed along the banks of the Rio Santa, up to about 300 m upstream, deposited in swales between rows of potato plants. Along the river bank, mud underlay the sand, suggesting that the river backed up before the maximum tsunami surge transported sand along these furrows. This river backup is consistent with eyewitness accounts collected by a Peruvian quick-response team (OCALA, 1998).

Tsunami Modeling

We performed numerical modeling of this event using the shallow-water-wave code VTCS-3 of TITOV and SYNOLAKIS (1997). For modeling purposes, four on-land profiles, measured down to the shoreline, were matched to nearshore:shelf bathymetry from maps. The bathymetry used for the computations was 5-min data (a 9-km grid) corrected using nautical charts and then interpolated down to a 600-m grid in the nearshore area. As a result of this coarse grid, small-scale features of the nearshore bathymetry were not captured, and inundation computations would have been meaningless. Instead, VTCS-3 was used to perform 10-m depth threshold computations (see TITOV and SYNOLAKIS, 1997), except where detailed surface transect measurements were made, and thus where 1-D resolution profiles were available, allowing reliable inundation computations.

For our model (see also TITOV and SYNOLAKIS, 1998) the source mechanism (Fig. 3) was approximated as a double-couple model with a single rectangular plane rupture, and as per the preferred Harvard CMT solution. The size and location of the fault rupture were estimated from the distribution of aftershocks. Several trial computations were performed, changing slightly the location (source geometry) and average slip amount of the source to obtain a distribution of computed wave heights similar to the measured runup heights, as is now standard with field-data simulations. The final source parameters used were L 120 km, W 60 km, strike 340°, dip 15°, rake 96°, U 4 m, and produced static displacement of the sea floor with maximum uplift of 1.8 m and maximum subsidence of 0.7 m.

If an M_w of 7.5 is applied to our analysis, a calculated rigidity of 0.75 10^{10} N: m^2 would be obtained, a relatively low value although similar to those suggested for tsunami earthquakes (see, e.g., SYNOLAKIS *et al.*, 1997; however note that in this paper they misquoted the estimate by an order of magnitude; HEINRICH *et al.*, 1998). A doubling of the rigidity (to 1.5, which most workers might consider more

realistic) would require either a minor difference in moment magnitude, or a change in magnitude of displacement. Our analysis, relatively simple and originally completed in 1996, shortly after the event, produces results as good or better than HEINRICH *et al.* (1998) (see also IHMLÉ *et al.*, 1998; their parameters: 110 km 40 km, U 2.3 m; 0.9, 0.4 m water displacement, rigidity 2.1 10^{10} N:m^2; moment 2.1 10^{20} N:m^2; they had access to and cited an earlier version of this manuscript). With our parameters, the calculated seismic moment would be 2.16 10^{20} Nm, consistent with the Harvard estimate of 2.2 10^{20} (the USGS estimate was 1.1 10^{20}). HEINRICH *et al.* (1998) and IHMLÉ *et al.* (1998) argue, based on their seismic analysis, that the proper modulus of rigidity for this event was higher than the low values typical for tsunami earthquakes (see also NEWMAN and OKAL, 1996).

Some workers have argued that it is preferable to use the seismic source inversion of the event (as in IHMLÉ *et al.*, 1998) as input to the tsunami model (as in HEINRICH *et al.*, 1998). This argument may well be true, from a strictly scientific standpoint. However, time is needed to produce such a model, and yet IHMLÉ *et al.*'s resultant source produces runup distribution (HEINRICH *et al.*) not noticeably better than the simplest source model that uses only CMT solution parameters (available almost in real time). Tsunami runup models themselves do not appear to differentiate between these two source specifications.

Our source model produces a leading depression wave which propagates toward the shoreline in the area between Huanchaco and Huarmey. Outside this area, the computations suggest a leading-elevation wave. This result is consistent with eyewitness observations and tide-gauge data to the north, but inconsistent with the tide-gauge record at Callao to the south, which shows a leading depression, and the eyewitness at Puerto Supe, who noted that the water went out first. This inconsistency does not, however, negate the general fit of the model to the area experiencing significant runup.

Very quickly after initial wave generation in the model, the sea surface forms a long-crested wave almost parallel to the shoreline. Shown in Figure 3 is a comparison between computed tsunami heights and runup measurements. There are two locations where discrepancies are especially large, based on using the 600-m bathymetric data (HEINRICH *et al.*'s, 1998 model was no more successful). First, runup at Culebras was measured as high as 5 m; however, note that Culebras (Fig. 1) is located at the deepest point of a small cove and has a relatively steep shoreline, hence the tsunami might have been focused by local bathymetry. Also, this measurement was not rated highly reliable (see Table 3 and Appendix B), and the high runup was measured in a small gully and may be a very localized splash, which a 600-m grid resolution cannot reproduce. Second, our field data near Trujillo exhibit a distinct local maximum in runup distribution, which is not simulated by our computations; these numbers are also based on eyewitnesses without corroborating physical evidence (see Table 3, Appendix B). Even computations with

different single source locations and sizes did not significantly change the predictions in this area, consequently we conjecture that wave refraction due to sub-600-m scale features is important here. However, if the reported runups are reliable, another possible explanation might be complex source motions with multiple subfaults, although IHMLÉ *et al.* (1998) conclude a fairly simple rupture. Studies with higher resolution bathymetric data may be necessary to resolve the sources of discrepancies.

We use so-called threshold computations to model Peru tsunami propagation (see also TITOV and SYNOLAKIS, 1998). This type of model inevitably underestimates runup values. An amplification factor is commonly applied to compensate for runup amplification, because the inundation process, which amplifies runup amplitudes, is not computed in a threshold model. The increase of a tsunami amplitude from 10-m depth (or any other threshold depth) to the runup inundation level depends on many factors, including local bathymetry and topography, and tsunami wavelength, amplitude and shape; therefore amplification factors can be very inconstant along a complex shoreline (TITOV and SYNOLAKIS, 1997). The amplification factor can vary from 1 to 5 (or more, depending on the threshold depth) and it is difficult to anticipate the proper value *a priori*. The 1-D inundation computations in four locations, as described below, were performed in part to estimate the amplification of the runup. The inundation computations did not produce larger runup values than the threshold model estimates. Therefore, there is no (*a priori*) reason to apply any amplification factors to the computed runup estimates on Figure 3.

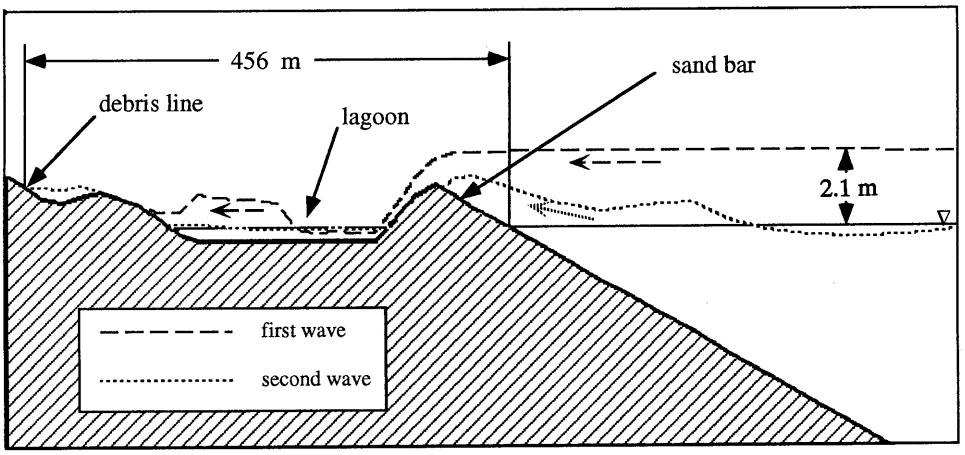

Figure 4
Tsunami water-surface profiles at Campo Santa, simulated by the two-dimensional model (see also TITOV and SYNOLAKIS, 1998).

Figure 4 shows results of runup computations using a hybrid inundation and threshold hydrodynamic computation, as used for the 1992 Nicaraguan tsunami (TITOV and SYNOLAKIS, 1993; see also TITOV and SYNOLAKIS, 1998, 1997). High-resolution bathymetric data are only available for four sites, thus we used the 2-D wave profile as calculated at the 100-m depth contour (where its crest was everywhere parallel to the shoreline), as input into a 20-m-grid resolution, 1-D inundation calculation. The inundation predictions are similar to those predicted by threshold calculations, not entirely unexpected, as threshold calculations work adequately when modeling small waves over gentle beaches with no longshore or onshore variation. However, the inundation computation produced the shoreline evolution dynamics; Figure 4 delineates the process of the tsunami climbing up the beach in Campo Santa. The measured 455-m penetration distance and 1.21-m runup height were modeled as 500 m and 1.8 m, respectively. At Rio Santa, the measured 364-m penetration and 3.2-m runup height were computed as 390 m and 3.4 m, respectively. Computed flow velocities in Campo Santa over the sand bar are 2.8 m:sec for the first wave (amplitude 0.96 m above the bar crest) and 4.3 m:sec (about 10 mi:hr, or 8.4 knots) for the second (0.8 m above the bar). On the back (land) side of the bar the maximum water speed is calculated as 6.6 m:sec (15 mi:hr, or 13 knots). This is consistent with Okushiri simulations (TITOV and SYNOLAKIS, 1997), which showed peak velocities on the back side of the overtopped land spit. Velocities at Okushiri were considerably higher (up to 19 m:sec), because the event was of much greater scale (wave height over the spit was about 10–15 m).

Having participated in many field surveys, we want to admonish modelers to use reported runup data with caution, and not to attempt detailed matches with all data, for several reasons. For example, eyewitnesses commonly exaggerate reports due to the traumatic nature of the event, and their desire to impress surveyors. Local topography and structures such as walls and houses can dramatically affect local runup. Also, some reported numbers are not runup (elevation at maximum inundation) but are the measured elevation of surges over beach ridges, focused between high spots, and other features. As PELAYO and WIENS (1990) argued for the 1960 event, we do not think a landslide can explain, or should be invoked to explain, the 1996 Peru runups or runup discrepancies; overall, they are consistent with a double-couple model of a (borderline) tsunami (slow, shallow) earthquake.

Discussion

As noted earlier, a tsunami on a coastal desert may be difficult to compare to other events, both in terms of measured runup data and in terms of cost to human lives and structures. Our field observations of the Chimbote 1996 tsunami suggest that this event is similar in origin and scale to the Peru 1960 event (PELAYO and WIENS, 1960) and the Nicaragua 1992 event (SATAKE *et al.*, 1993), as might have

been anticipated, based on similar magnitudes (Chimbote: earthquake magnitudes M_s 6.6 and M_w 7.5; tsunami magnitude, M_t 7.8; 1960 Peru, M_s 6.75, M_w 7.6, M_t 7.75; Nicaragua, M_s 7.2, M_w 7.6, M_t 8.0). In our post-tsunami survey, the Nicaragua event appeared far more devastating, and indeed it did destroy many more houses, and generated more than ten times as many casualties. Also, the highest reported "runup" measurements from Nicaragua were primarily from marks on trees and houses, rather than maximum inundation elevations (see below). The 1996 Peru tsunami was slightly smaller than Nicaragua, but the differences have significantly more to do with the differences between the coastlines. The 1960 and 1996 Peru events produced significantly less damage and fewer casualties than the 1992 Nicaragua, however Peru's hyperarid coastline is considerably more sparsely populated.

Our threshold simulations demonstrate that local runup heights can be hindcast from simple seismic parameters for the Chimbote earthquake. Overall, better agreement has been obtained between field measurements and hydrodynamic data for this event than with most models for Nicaragua, whether using threshold or combinations of threshold and inundation computations. We believe that this agreement is partly the result of coastal conditions in Peru, where there are very few structures and little or no vegetation along the coastline. These conditions necessitated measurement of wrack lines at maximum inundation, rather than relying on marks on houses or trees, on beach crests. Inundation codes predict the elevation of maximum inundation (runup, as formally defined), consequently these predictions agree better with inundation than with maximum height measurements. In Nicaragua, most measurements were tsunami heights at or near beach crests; and even when both measurements were available, the larger values were commonly used for comparison with model results. For example, at Playa de Popoyo, Nicaragua, a site topographically comparable to many observed in Peru, the average tsunami elevation over the beach crest was about 4.5 m (range 3.2 to 5.6 m), whereas the runup (elevation at maximum inundation) averaged only about 2 m (range 1.5 to 2.2 m) (J. Bourgeois, field notes, 1992 and 1993). If one assumes, as was observed in Nicaragua and has been observed elsewhere (Katsayuki Abe, written communication), that maximum tsunami height is typically about twice the elevation at maximum inundation (runup), then the hydrodynamic characteristics of this Chimbote 1996 event are also comparable locally to the 1992 Nicaragua earthquake.

The 1960 (PELAYO and WIENS, 1990) and 1996 northern Peru subduction-zone earthquakes fall into the category of tsunami earthquakes. The February 1996 event bears all the basic characteristics (PELAYO and WIENS, 1992), including the one that most concerns local populations: the earthquake was only weakly felt. It seems possible that the entire northern part of the Peru subduction zone could produce these kinds of events—slow, shallow, tsunamigenic earthquakes near the tip of the subduction zone. In northern Peru, characteristics on land (lack of uplift) and

offshore (wide shelf, relatively high sediment supply) tend to support the idea that this subduction zone segment is only weakly coupled. In order to improve our understanding of tsunami earthquakes, and our ability to predict where they are likely to occur, it is imperative to examine closely these recent events, such as Nicaragua 1992 and Peru 1996.

The region between the 1960 and 1996 Peru events has not had a subduction-zone earthquake since at least 1619 (if we and others are correct in our interpretation of that event). Yet, even though the 1960 and 1996 events produced more casualties than other recent tsunamis in southern Peru, tsunami hazard planning has been focused on the south, due to its history of more frequent events. The 1996 Chimbote tsunami is one of several recent events that are wake-up calls to the hazard planning community.

Acknowledgments

We gratefully acknowledge the financial support of the U.S. National Science Foundation, which provided the principal funding for this project; and the support and cooperation of the Peruvian Navy (office of Hydrography and Navigation; particularly Hector Soldi, Guillermo Hasembank), the Geophysical Institute of Peru (particularly Leonidas Ocala), the Peruvian Institute of National Civil Defense (particularly Mateo Casaverde), and the National University of Engineering during the period of this survey. Two anonymous reviewers, one in particular, provided constructive feedback and helped us generate a more synthetic picture of the northern Peru subduction zone. We are also grateful for suggestions and enthusiastic encouragement from Renata Dmowska.

Dr. Titov's contribution to this paper was funded in part by the Joint Institute for the Study of the Atmosphere and Ocean (JISAO) under NOAA Cooperative Agreement No. NA67RJ0155, Contribution number 583. The views expressed therein are those of the author(s) and do not necessarily reflect the views of NOAA or any of its subagencies.

Appendix A

Historic large and destructive earthquakes and other tsunamigenic events originating off Peru north of 12°S (see summary of data, in Table 1, main text). Summaries compiled primarily from DORBATH *et al.* (1990), LOCKRIDGE (1985), SWENSON and BECK (1996), and CARBONEL and AGUIJE (1989). All except 1970 (and possibly 1725) are interpreted as subduction-zone (interplate) events.

19 February 1619: (DORBATH *et al.*, 1990). Earthquake destroyed Trujillo. SILGADO (1978) notes an account of muddy waters inundating (coastal) towns

(Santa, Barranca, others), attributed to river flooding, but we think suggestive of tsunami. WELLS *et al.* (1987) reported a wood debris line on Santa delta, which they interpreted as tsunami-generated (see text). Not mentioned in Lockridge tsunami catalogue or in Swenson and Beck.

17 June 1678: (DORBATH *et al.*, 1990) Area north of Lima most severely shaken. A tsunami threw little boats inland near Santa, according to the testimony of a British officer who went there a few years later (Parish, 1836, cited in Dorbath *et al.*); no references found to tsunami at Callao, but another witness confirmed its occurrence at Pisco (1728 reference cited in Dorbath *et al.*). Not reported in Silgado, Lockridge or Swenson and Beck.

25 January 1725: (DORBATH *et al.*, 1990). Dorbath *et al.* postulate earthquake was similar to 1970 event; damage primarily along coast; Huascaran glacier collapse, with 1,500 deaths at Yungay, prefiguring 1970. No tsunami documented. Not in Lockridge or Swenson and Beck.

28 October 1746: (DORBATH *et al.*, 1990; SWENSON and BECK, 1996). Earthquake ruptured same area as 1940 and 1966 events, as well as part of 1974 event; the 1746 event interpreted as a multiple asperity rupture (Swenson and Beck). Worst earthquake ever to hit Lima; towns north to 10°S razed or badly damaged, and down to Canete (approx. 13.5°S). Half an hour after main shock, tsunami flooded and virtually flattened Callao (3,800 of 4,000 died there); principal wave >20 m high, entered more than 5 km inland; 19 ships sunk, 4 washed over town; ''Callao was a confused accumulation of sand and gravel''; ports severely damaged all along the coast (Dorbath *et al.*). Tsunami also destroyed towns of Guanape, Santa, Chancay, and Pisco, Peru; Concepcion, Chile (Lockridge). No mention of this tsunami found in Japan (Swenson and Beck); noted in Acapulco (Lockridge).

24 May 1940: (DORBATH *et al.*, 1990; SWENSON and BECK, 1996; LOCKRIDGE, 1985). Originally interpreted as within downgoing plate; reinterpreted by Beck and Ruff (see Swenson and Beck) as shallow underthrusting event; hence entire plate boundary between 10 and 14°S has failed in this century (see Swenson and Beck). Dorbath *et al.* argued to move epicenter 1 degree west (i.e., to $\sim$78.2) based on isoseismals, and argued that focal mechanism indicates a fault plane dipping 25° ENE, ''…clearly…interplate event….'' Local tsunami runup 2–3 m; none in Japan.

13 January 1960: [Not in Table 1] Reported earthquake source (mag. 7.8) on land. LOCKRIDGE (1985) reports 5.7 m runup at Ancon (11.78°S), but no damage. Spurious report? Landslide?

20 November 1960: (PELAYO and WIENS, 1990; CARBONEL and AGUIJE, 1989). See text for earthquake discussion. Tsunami Callao 0.7 m amp.; Chimbote 0.91 m amp. (CARBONEL and AGUIJE); runup 1.2 m (Lockridge). Tsunami damage in Pimentel, Puerto Eten, Santa Rosa, San Jose, Lobos de Afuera Is. (devastated). Some unusually high runup reports in Lockridge. Teletsunami recorded in Hilo, 0.1 m; Japan, 0.15–0.34 m (Lockridge). Not reported or discussed in Dorbath *et al.*, Swenson and Beck.

17 October 1966: (DORBATH *et al.*, 1990; SWENSON and BECK, 1996; LOCKRIDGE, 1985; CARBONEL and AGUIJE, 1989). Tsunami 3.4 m amplitude in Callao, 1.18 m amp. in Chimbote; Callao tide-gauge record reproduced (in Carbonel and Aguije). Tsunami refraction diagram and tide-gauge record for Callao in KUROIWA (1995). Tsunami damage at Galapagos Is. (3-m runup), Trujillo (3 m), Casma ($2 million damage); Culebras, Puerto Chimu, Tortuga (''serious damage'' to these three); Callao (2.1-m runup); ''towns flooded'': Huara, Trujillo (presumably its coastal communities) Huacho, Ancon; other small runups noted north to Talara (0.1 m), south to Lebu, Chile (0.3 m) (Lockridge). Teletsunami recorded in Hawaii (0.27–0.37 m); Crescent City (0.06 m); Japan (0.15–0.38 m) (Lockridge).

31 May 1970: DORBATH *et al.* (1990) and SWENSON and BECK (1995) do not discuss at length because this is classified as a normal-fault event, not a subduction-zone event; Swenson and Beck (Fig. 20) map aftershock areas in two patches between coast and trench. This earthquake was very destructive, and includes the Huascaran slide catastrophe; 10s of thousands killed. Tsunami on Callao tide-gauge record reproduced in Carbonel and Aguije (1989, Fig. 3-3b), who also list some aftershocks that produced tsunamis measured on tide gauges (m's amplitude):

		EQ magnitude*	Callo	Chimbote
Main shock	31 May	7.8 (M_s)	1.13 m	– #
	31 May	5.6 (m_b)		1.13 m
	1 June	5.8–6.0 (m_b)	0.67 m	–
	2 June	5.7 (m_b)	0.24 m	–
	2 July	5.8 (m_b)	–	0.22 m

* Magnitudes as reported in USGS NEIC catalogue.
\# Not recorded, pen left paper.

3 October 1974: (DORBATH *et al.*, 1990; SWENSON and BECK, 1996; LOCKRIDGE, 1985; CARBONEL and AGUIJE, 1989). Earthquake occurred in ''seismic gap'' between 1940 and 1942 events, primarily to south of 12°S; aftershocks 240 km 50 km, parallel to trench; majority of moment release in NW half of aftershock zone; event ruptured bilaterally, 40 km to NW and 60 km to SW of epicenter. Callao tsunami amplitude 1.58 m; Chimbote ampl. 0.68 m; Callao tide-gauge record (Fig. 3-4a in Carbonel and Aguije). Tsunami refraction diagram and Callao tide-gauge record reproduced in Kuroiwa, 1995. Teletsunami recorded in Hawaii (0.37 m); Midway Is. (0.6 m); Crescent City (0.15 m), Wake Island (0.06 m), Am. Samoa (0.3 m) (Lockridge).

20 May 1978: (CARBONEL and AGUIJE, 1989). Tsunami Callao ampl. 0.45 m; Chimbote 1.28 m (Carbonel and Aguije). Not reported in Lockridge; Dorbath *et al.* or Swenson and Beck.

21 February 1996: See this paper; IHMLÉ *et al.* (1998); HEINRICH *et al.* (1998).

Appendix B

Notes on localities (S to N) where runup was measured (see Table 3; Figs. 1 and 3) [techniques used in square parentheses; surveying rods used for all vertical elevation].

Puerto Supe: A steep beach, small harbor, local pier. Navy officer, eyewitness; indicated point (along pier) to which water went out, and to point to which it came up. No clear physical evidence [hand level, tape].

Balnearia Tomborero: A steep, sandy pocket beach. Local guardian, eyewitness; pointed to where water rose. No obvious physical evidence [transit].

Huarmey: Pier and inlet along a marshy area at south end of long beach (north of headland); port captain's office and fish meal plant. Moderately reliable physical evidence—debris [hand level, pacing, distance estimated].

Tuquillo: Low sea wall along pocket beach; physical evidence (water marks inside hut) and eyewitnesses [hand level, tape].

Culebras: Complex small inlet and harbor. Equivocal physical evidence on local hillslope at south end of inlet (highest measurement); unreinforced wall near south end of inlet was pushed over; eyewitness accounts of water washing over dock in interior of inlet [hand level, tape].

Puerto de Casma: No details noted [hand level, tape].

Los Pinos: Runup 3 m on steep rock slopes; 1.8 m on flat part of beach; eyewitness pointed to tsunami mark, "a little above high tide mark" [hand level, tape].

Playa Tortuga: Small bay, rocky beach. Eyewitness reports that water overtopped pier; eyewitness pointed to sill where water reached on house [hand level, tape].

Playa Chimus: North end of long pocket beach, measurements at town just south of headland. Eyewitness description—very detailed, with some corroboration; physical evidence scant; water came up to but not over concrete soccer surface; locally, water washed over beach ridge and flowed down into town [transit, profile].

Playa Mar Brava: Long, straight, steep sandy beach south of (not too close to) a headland. No inhabitants; clear physical evidence—sand transport, debris line [two profiles measured, one with hand level, other with transit—Playa Mar Brava II].

Ensenada La Posa: Steep, gravelly pocket beach on west side of prominent headland. No inhabitants; clear physical evidence—debris lines [hand level and tape, several short profiles measured].

El Dorado: South side of tombolo, western end of long beach, relatively low relief, steepening toward headland; small habitation, restaurant. Eyewitnesses and some physical evidence (including boats washed inland) [hand level for elevation, estimated distance to boats].

Playa Alconsillo: Toward east end of tombolo; long, low beach, sand dunes. Physical evidence: debris line on local knoll [hand level, tape].

Chimbote Bay and Port of Chimbote: Heavily industrialized area, particularly toward north end of bay; docks, sea walls, etc. Interviews—many eyewitnesses, and some physical evidence [hand level, tape].

Coishco: Just north of headland, south end of long, moderately steep beach; fishing village, many structures. Interviews—many eyewitnesses, and physical evidence; damage to houses and fish-meal factory walls; already some repairs and changes since event [hand level and tape; transit profile at south end of town, near fish market].

Puerto Santa: Just north of headland, at south end of long, low beach with local marshes. Eyewitnesses and physical evidence—debris line, tsunami deposits [transit; profile].

Rio Santa: At mouth of Santa River, broad, low delta plain; low-relief intertidal zone, steep gravel beach with local beach scarp, then low-relief supratidal area (locally cultivated). Clear physical evidence (debris lines) and eyewitnesses; thin tsunami deposit; erosion along edge of river channel, upstream of mouth [profile measured with transit; Rio Santa III with hand level and tape].

Campo Santa: Broad accretionary plain north of mouth of Rio Santa; gravel beach ridges with swales and lagoons in between; current beach is steep, predominantly coarse sand. Clear physical evidence (debris line), eyewitness corroborated [profile measured by transit for elevations and most distances, with estimate of distance across lagoon, corroborated with GPS].

Bocana de Chao: River mouth and broad accretionary beach; physical evidence (debris lines) [transit Bocana de Chao II; hand levels, pacing Bocana de Chao I].

El Carmelo: Mouth of Viru River, coastal plain. Debris line, eyewitness; tsunami deposits [hand level, tape].

Las Delicias: Resort with sea walls. Eyewitnesses say tsunami came over wall, into swimming pool; no clear physical evidence [hand level, tape].

Huanchaco, *La Posa Huanchaco:* Long, moderately steep beach, beach resort, some structures. Eyewitnesses seem reliable; no clear physical evidence [transit at La Posa Huanchaco, hand level at Huanchaco].

Huaca Prieta: Long, gravelly beach. Eyewitnesses inconsistent about earthquake, but consistent enough that tsunami locally went over top of beach ridge [transit].

Puerto Chicama: Moderately long, moderately steep beach, some structures. Eyewitnesses; no clear physical evidence [transit].

REFERENCES

ABE, KA. (1979), *Size of Great Earthquakes of 1873–1974 Inferred from Tsunami Data*, J. Geophys. Res. *84*, 1561–1568.

ABE, KA. (1981), *Physical Size of Tsunamigenic Earthquakes of the Northwestern Pacific*, Phys. Earth Planet. Inter. *27*, 194–205.

ABE, KA. (1996), *Tsunami Magnitude of the 21 February 1996 Peru Event;* E-mail communication via the tsunami bulletin board.

ABE, KU., ABE, KA., TSUJI, Y., IMAMURA, F., KATAO, H., IIO, Y., SATAKE, K., BOURGEOIS, J., NOGUERA, E., and ESTRADA, F. (1993), *Field Survey of the Nicaragua Earthquake and Tsunami of September 2, 1992*, Bull. Earthq. Res. Inst., Univ. of Tokyo *68*, 23–70.

ATLAS DEL PERU (1989), Chief editor, *Carlos Penaherrera del Aguila*; published by the Instituto Geografico Nacional.

BECK, S. L., and RUFF, L. J. (1989), *Great Earthquakes and Subduction along the Peru Trench*, Phys. Earth Planet. Interiors *57*, 199–224.

CHAUCHAT, C., *Early hunter gatherers on the Peruvian coast*. In *Peruvian Prehistory* (Keating, R. W., ed.) (Cambridge Univ. Press 1987) pp. 41–66.

CARBONEL, H. C., and AGUIJE, CH. (1989), *Sobre el peligro de inudacion por maremotos en las costas de Lima y Ancash*, Informe tecnico, Inst. Geof. de Peru.

DEWEY, J. F., and LAMB, S. H. (1992), *Active Tectonics of the Andes*, Tectonophysics *205*, 79–95.

DE VRIES, T. J. (1988), *The Geology of Marine Terraces (tablazos) of Northwest Peru*, J. South American Earth Sci. *1*(2), 121–136.

DORBATH, L., CISTERNAS, A., and DORBATH, C. (1990), *Assessment of the Size of Large and Great Historical Earthquakes of Peru*, Bull. Seismol. Soc. Am. *80*(3), 551–576.

EKSTRÖM, G., and SALGANIK, G. (1996), *Harvard CMT Solution for 21* Feb. *96* Earthquake off the Coast of Northern Peru (via Internet).

HASEGAWA, A., and SACKS, I. S. (1981), *Subduction of Nazca Plate Beneath Peru as Determined by Seismic Observations*, J. Geophys. Res. *86*, 4971–4980.

HEINRICH, P., SCHINDELE, F., and GUIBOURG, S. (1998), *Modeling of the February 1996 Peruvian Tsunami*, Geophys. Res. Lett. *25*, 2687–2690.

HSU, J. T., LEONARD, E. M., and WEHMILLER, J. F. (1989), *Aminostratigraphy of Peruvian and Chilean Quaternary Marine Terraces*, Quat. Sci. Rev. *8*, 255–262.

KANAMORI, H. (1972), *Mechanism of Tsunami Earthquakes*, Phys. Earth Planet. Inter. *6*, 246–259.

KUROIWA, J. (1995), *Tsunamis: Population Evacuation and Land Use Planning for Disaster Mitigation, Localities Studied in Peru (1981–1994)*, U.N. International Decade of Natural Disaster Reduction Publication (original in Spanish; revised by D. Zupka, translated by C. V. Schneider), 46 pp.

LANGER, C. J., and SPENCE, W. (1995), *The 1974 Peru Earthquake Series*, Bull. Seismol. Soc. Am. *85*(3), 665–687.

LINDO, R., DORBATH, C., CISTERNAS, A., DORBATH, L., OCOLA, L., and MORALES, M. (1992), *Subduction Geometry in Central Peru from a Microseismicity Survey: First Results*, Tectonophysics *205*, 23–29.

LOCKRIDGE, P. A. (1985), *Tsunamis in Peru–Chile*, World Data Center A for Solid Earth Geophysics Report SE-39, 97 pp.

LOMNITZ, C. (1970), *Major Earthquakes and Tsunamis in Chile during the Period 1535 to 1955*, Geolog. Rundsch. *59*, 938–960.

MACHARE and ORTLIEB (1992), *Plio-Quaternary Vertical Motions and the Subduction of the Nazca Ridge, Central Coast of Peru*, Tectonophysics *205*, 97–108.

NEWMAN, A. V., and OKAL, E. A. (1996), *Source Slowness of the February 21, 1996 Chimbote Earthquake Studied from Teleseismic Energy Estimates*, EOS *77*(17), S184.

NORABUENA, E., SNOKE, J. A., and JAMES, D. E. (1994), *Structure of the Subducting Nazca Plate beneath Peru*, J. Geophys. Res. *99*, 9215–9226.

NORABUENA, E., LEFFLER-GRIFFEN, L., MAO, A., DIXON, T., STEIN, S., SACKS, I. S., OCOLA, L., and ELLIS, M. (1998), *Space Geodetic Observations of the Nazca-South America Convergence across the Central Andes*, Science *279*, 358–362.

OCALA, L. C., *Effects of February 21, 1996, Chimbote tsunami*. In *Modern Preparation and Response for Earthquake, Tsunami and Volcanic Hazards*, International Conference 27–30 April, 1998 (Santiago, Chile 1998) 267 pp.

OKAL, E. A. (1988), *Seismic Parameters Controlling Far-field Tsunami Amplitudes: A Review*, Natural Hazards *1*, 67–96.

PELAYO, A. M., and WIENS, D. A. (1990), *The November 20, 1960 Peru Tsunami Earthquake: Source Mechanism of a Slow Event*, Geophys. Res. Lett. *17*, 661–664.

PELAYO, A. M., and WIENS, D. A. (1992), *Tsunami Earthquakes: Slow Thrust-faulting Events in the Accretionary Wedge*, J. Geophys. Res. *97*, 15,321–15,337.

SATAKE, K., BOURGEOIS, J., ABE, KU., ABE, KA., TSUJI, Y., IMAMURA, F., IIO, Y., KATAO, H., NOGUERA, E., and ESTRADA, F. (1993), *Field Survey of the Nicaragua Earthquake and Tsunami of September 2, 1992*, EOS, Trans. AGU *74*, 145 and 156–157.

SATAKE, K., and IMAMURA, F., eds. (1995), *Tsunamis 1992–94*, Pure appl. geophys. *144*(3:4).

SILGADO, E. (1978), *Historia de los sismos mas notables ocurridos en el Peru (1513–1974)*, Inst. Geol. Min., Lima, 131 pp.

STOKER, J. J., *Water Waves* (Interscience Publishers, Inc., New York 1957) 567 pp.

SWENSON, J. L., and BECK, S. L. (1996), *Historical 1942 Ecuador and 1942 Peru Subduction Earthquakes, and Earthquake Cycles along Colombia–Ecuador and Peru Subduction Segments*, Pure appl. geophys. *146*(1), 67–101.

SYNOLAKIS, C. E., LIU, P., CARRIER, G., and YEH, H. (1997), *Tsunamigenic Sea-floor Deformations*, Science *278*, 598–600.

TITOV, V. V., and SYNOLAKIS, C. E., *A numerical study of the 9:1:92 Nicaraguan Tsunami*, Proceedings of the IUGG:IOC International Tsunami Symposium, Wakayama, Japan. (Japan Soc. Civil Engineers 1993) pp. 585–598.

TITOV, V. V., and SYNOLAKIS, C. E. (1997), *Extreme Inundation Flows during the Hokkaido–Nansei–Oki Tsunami*, Geoph. Res. Lett. *24*(11), 1315–1318.

TITOV, V. V., and SYNOLAKIS, C. E. (1998), *Numerical Modeling of Tidal Wave Runup*, J. Waterway, Port, Coastal and Ocean Engineering *124*(4), 157–171.

TUSHINGHAM, A. M., and PELTIER, W. R. (1991), *Ice-3G: A New Global Model of Late Pleistocene Deglaciation Based Upon Geophysical Prediction of Post-glacial Relative Sea Level Change*, J. Geophys. Res. *96*, 4497–4523.

WELLS, L. E. (1990), *Holocene History of the El Niño Phenomenon as Recorded in Flood Sediments of Northern Coastal Peru*, Geology *18*, 1134–1137.

WELLS, L. E. (1996), *The Santa Beach Ridge Complex: Sea-level and Progradational History of an Open Gravel Coast in Central Peru*, J. Coastal Res. *12*(1), 1–17.

WELLS, L. E., DE VRIES, T. J., and QUINN, W. H. (1987), *Driftwood Deposits of the 1618 A. D. Tsunami, Northern Coastal Peru*, Geol. Soc. Am. Abstr. w. Programs, *19*(7), 885.

(Received May 13, 1998, revised December 30, 1998, accepted February 3, 1999)